Bone structural characteristics and response to bisphosphonate treatment in children with Hajdu-Cheney Syndrome

Sakka, Sophia; Gafni, Rachel I; Davies, Justin; Clarke, Bart; Tebben, Peter ; Samuels, Mark; Saraff, Vrinda; Klaushofer, Klaus; Fratzl-Zelman, Nadja; Roschger, Paul; Rauch, Frank; Högler, Wolfgang

DOI:
10.1210/jc.2017-01102

Bone structural characteristics and response to bisphosphonate treatment in children with Hajdu-Cheney Syndrome

Sophia Sakka[1], Rachel I. Gafni[2], Justin H. Davies[3], Bart Clarke[4], Peter Tebben[4], Mark Samuels[5], Vrinda Saraff[1], Klaus Klaushofer[6], Nadja Fratzl-Zelman[6], Paul Roschger[6], Frank Rauch[7], Wolfgang Högler[1,8]

[1] Department of Endocrinology and Diabetes, Birmingham Children's Hospital, Birmingham, UK

[2] Section on Skeletal Disorders and Mineral Homeostasis, NIDCR, National Institutes of Health, Bethesda, Maryland, USA

[3] Department of Endocrinology, Southampton Children's Hospital, Southampton, UK

[4] Department of Internal Medicine, Division of Endocrinology, Diabetes, Metabolism, and Nutrition, Mayo Clinic College of Medicine, Rochester, Minnesota, USA

[5] Centre de Recherché du CHU Ste-Justine, and Department of Medicine, Université de Montréal, Montreal, Canada

[6] Ludwig Boltzmann Institute of Osteology at Hanusch Hospital of WGKK, Vienna, Austria and AUVA Trauma Centre Meidling, 1st Med. Dept., Hanusch Hospital Vienna, Austria;

[7] Shriners Hospital for Children and McGill University, Montreal, Quebec, Canada

[8] Institute of Metabolism and Systems Research, University of Birmingham, Birmingham, UK

Abbreviated title: Bone quality and treatment in Hajdu-Cheney Syndrome

Keywords: Hajdu-Cheney Syndrome, bone density, NOTCH2, bisphosphonates, bone biopsy, pQCT

Word count: 3532 words

Number of Figures and Tables: 3 Figures and 3 Tables

Corresponding Author and person to whom reprint should be addressed:

Dr Wolfgang Högler

Department of Endocrinology and Diabetes,

Birmingham Children's Hospital, Birmingham,

Steelhouse Lane

B138LN

United Kingdom

Fax: ++441213338191

Email: wolfgang.hogler@bch.nhs.uk

Disclosure summary: The authors have nothing to disclose.

Abstract

Context: Hajdu-Cheney syndrome (HJCYS) is a rare, multisystem, bone disease caused by heterozygous mutations in the *NOTCH2* gene. Histomorphometric and bone ultrastructural analyses in children have not been reported and sparse evidence exists on response to bisphosphonate (BP) therapy.

Objective: To investigate clinical and bone histomorphometric characteristics, bone matrix mineralization and the response of bone geometry and density to BP therapy.

Patients: Five children with HJCYS (3 males) aged between 6.7 and 15.3 years.

Interventions: Various BP regimens (pamidronate, zoledronic acid, alendronate) were used for between one and ten years.

Main Outcome Measures: Pre-treatment transiliac bone biopsy specimens and peripheral quantitative computed tomography (pQCT) results were available in four and three subjects, respectively. Bone histomorphometry and quantitative backscattered electron imaging were performed in two patients. The response to BP was monitored using dual energy X-ray absorptiometry and pQCT.

Results: Three patients had novel *NOTCH2* mutations. Histomorphometry demonstrated increased bone resorption and osteoclast numbers, increased heterogeneity of mineralization and immature, woven bone. Trabecular bone formation was normal or elevated. Radius cortical thickness and density and lumbar spine bone mineral density were reduced at baseline and increased in response to BP therapy, which was not sustained after therapy discontinuation.

Conclusions: Increased bone resorption and low cortical thickness are consistent with the effect of activating *NOTCH2* mutations, which stimulate osteoclastogenesis. The increase in lumbar spine bone density and radial cortical thickness and density by BP therapy provides evidence of beneficial treatment effects in children with HJCYS.

Précis

High resorption, heterogenous mineralization, woven bone and low cortical thickness are characteristic of HJCYS bone. Reduced bone density and cortical thickness increased during bisphosphonate therapy.

Introduction

Hajdu-Cheney Syndrome (HJCYS) is a rare multi-system disorder with an autosomal dominant pattern of inheritance, characterized by acroosteolysis, osteoporosis, short stature, specific craniofacial features, neurological symptoms, cardiovascular defects and polycystic kidneys (1). The HJCYS phenotype was originally described by Hajdu in 1948 (2) and expanded by Cheney (3). Since then various sporadic or familial cases have been reported. HJCYS is caused by mutations in exon 34 of the *NOTCH2* gene, which encodes the Notch2 receptor, a regulator of skeletal development involved in osteoblast and osteoclast differentiation (4,5). The Notch2 receptor belongs to a family of four (Notch 1–4) transmembrane receptors that play a critical role in cell fate decisions. Notch1 and specifically Notch2 receptors are considered responsible for the skeletal effects (1,6).

NOTCH2 mutations in HJCYS result in a receptor protein lacking a predicted C-terminal proline-glutamic acid-serine-threonine-rich (PEST) domain, which normally reduces the half-life of the encoded protein. Absence of this domain is presumed to yield dominant gain-of-function effects through increased protein stability and signalling activity (4,5,7), although this has not yet been verified in functional studies of NOTCH2. The canonical NOTCH pathway is known to modulate cell fate and function in osteoblast and osteoclast lineages (1,8). In murine models, the activation of Notch signalling stops the commitment of pluripotent precursors to the osteoblastic lineage, and suppresses osteoblast differentiation (9). *Notch2* mutant mice carrying an equivalent truncating mutation deleting the putative PEST domain exhibit low bone mass secondary to increased osteoclast numbers and high bone resorption, shown by the increase in the preosteoclast cell pool, the osteoclastogenic response to receptor activator of nuclear factor KappaB ligand (Rankl), and tissue Rankl concentrations (10).

Whilst osteoporosis is a known feature of human HJCYS, little is known regarding the bone tissue characteristics. Early histological studies in adults were partly inconclusive (11-15). Several reports have documented histological features of high turnover osteoporosis, with increased resorptive surfaces and decreased endosteal bone surfaces compared with healthy controls (11-14). To date, histomorphometric and bone ultrastructural analyses in the developing skeleton of children with

HJCYS have not been reported. In addition, while sparse evidence suggests increasing bone mineral density (BMD) during bisphosphonate (BP) therapy in adults (15-19) and two children (20,21) with HJCYS, the differential response in bone geometry and density of the axial and appendicular skeleton has not been illustrated.

The aim of this study was to investigate clinical and histomorphometric characteristics, bone matrix mineralization and the response of bone geometry and density to BP therapy in five children with HJCYS, three of whom had novel *NOTCH2* mutations.

Materials and Methods

Patients

Five children (2 girls, 3 boys) with HJCYS presented to metabolic bone physicians in Birmingham/UK, Bethesda/USA, Southampton/UK, Rochester/USA and Montreal/Canada. Clinical information and radiographic data from skeletal surveys were collected at diagnosis. Patients 1, 2, 3 and 5 underwent genetic testing of the *NOTCH2* gene; patient 4 had a clinical diagnosis only. Sequencing was performed using standard methods and data were analyzed using MutationSurveyor (Soft Genetics, Inc). Trans-iliac bone biopsies were taken following informed consent. All were treated with various BP regimes with a starting age between 6.7 and 15.3 years, based on reduced BMD and/or vertebral and limb fractures. Informed consent for genetic studies and publication of clinical data was obtained from patients or their parents as appropriate.

Bone histomorphometry and quantitative Backscattered Electron Imaging (qBEI)

Patients 3 and 5 had transiliac bone biopsies taken before the initiation of BP treatment, following double-labelling with tetracycline to allow for dynamic measurement of bone formation. Samples were sent to the Genetics Unit of the Shriners Hospital for Children in Montreal, Canada. Sample preparation and histomorphometric analyses were performed using standard procedures (22). Results were compared to reference data of healthy age-matched controls (22,23). Subsequently, the residual blocks were prepared to assess bone mineralization density distribution (BMDD), reflecting the

calcium content of cortical and trabecular bone matrix by qBEI and compared to controls as described previously (24,25,26), at the Ludwig Boltzmann Institute of Osteology in Vienna, Austria.

Patient 1 also had a pre-treatment transiliac bone biopsy, and patient 4 had a post-treatment biopsy following 20 months of BP discontinuation. Whilst reports were available, the latter biopsy samples were either decalcified or not double-labelled, and not available for detailed histomorphometric analysis. Patient 2 had post-treatment, non-histomorphometric analysis of maxillary bone, as previously reported [subject HJCYS05 in (27)].

Dual energy X-ray absorptiometry (DXA)

Bone mineral density (BMD) of patient 1 was measured using a GE Lunar™ iDXA (GE Medical Systems, Madison, Wisconsin, US). Patients 2, 3 and 5 were scanned on a QDR Discovery Hologic™ (Hologic, Waltham, MA, US), and patient 4 had scans on both DXA models. Lumbar spine scans were obtained; iDXA scans were analysed using Encore version 13.6 (Basic and Enhanced) and Hologic scans with Apex 4.1. Lumbar spine BMD results were adjusted for body size by calculating the bone mineral apparent density (BMAD, g/cm^3) using the method of Carter et al (28) for GE scanner output, and by using height-adjusted Z-scores (HAZ) for Hologic scanner output (29).

Peripheral quantitative computed tomography (pQCT)

pQCT was performed at the distal and proximal radius of the non-dominant forearm (4% and 66% of radial length, respectively) using a Stratec XCT2000® scanner (Stratec Inc., Pforzheim, Germany) with voxel size 0.4 mm, slice thickness 2.3 mm and scan speed 25 mm/s. Positioning of the reference line depending on the presence of a growth plate was performed as previously described (30). Bone measurements were obtained 4 % proximal to the reference line for total and trabecular vBMD, and at the 66 % site for cortical vBMD, bone mineral content (BMC), muscle area and cortical thickness. Cortical thickness was calculated using the manufacturer's software. Image acquisition, processing and the calculation of numerical values were performed using the manufacturer's software package (XCT 6.0). Z-scores were calculated using reference data for the distal (30) and proximal (31,32)

radius. Patients 1, 3 and 5 had pQCT scans before commencing BP treatment. Repeat pQCT scans were performed in patient 1 four years after starting BP, and in patient 3 one and 4.5 years after starting BP.

Results

Patient clinical characteristics

All patients were born to healthy, non-consanguineous parents. Patients 1, 3 and 5 were found to have novel heterozygous protein-truncating *NOTCH2* gene mutations (reference sequence NM_024408.3): c.6902T>A (p.Leu2301*), c.6787C>T (p.Gln2263*) and c.6724_6725delAG (p.Ser2242*), respectively (mutations submitted to ClinVar). Patient 2's mutation was previously reported (27). In addition to displaying common features of HJCYS, our patients showed some rarely described (33) phenotypic features, such as intestinal malrotation, delayed puberty (P1 had late menarche age 19 years with normal oestradiol and LHRH test results) and hip acetabular dysplasia with loss of normal femoral epiphysis. Their median height Z-score was -1.4 (range -3.5 to -0.4). Patient 1 was wheelchair dependent, but patients 2-5 had normal mobility. **Supplementary Table 1** summarizes the genetic and phenotypic characteristics of all 5 patients, and **Supplementary Table 2** summarizes their radiological findings.

Treatment with BP

Patient 1 has been receiving 6-monthly intravenous zoledronate 0.05 mg/kg/dose from the age of 15 years. Patient 2 received 3-monthly intravenous pamidronate 1mg/kg/dose from age 6.8 years for 1 year, and then switched to 35 mg oral alendronate weekly for 3 years, which was increased to 70 mg weekly for 2.5 years. Following a 5-year interval without any BP treatment, he had one infusion of 5 mg zoledronate at the age of 17.5 years. Patient 3 received 3 doses of 6-monthly zoledronate 0.05 mg/kg/dose at the age of 15.5 years and then refused to have more infusions. Patient 4 started therapy at the age of 10 years with 5 mg oral daily alendronate, followed by 35 mg weekly from age 13 years, and 70 mg weekly from age 15 years, which was discontinued at age 20 years. Following a 2-year interval without treatment he had 2 more years of 70 mg weekly alendronate. He then stopped BP

therapy aged 24 years, due to declining glomerular filtration rate caused by polycystic kidney disease requiring renal transplantation at age 25 years. Patient 5 (10 years) has just started therapy with 4-monthly intravenous pamidronate 1.5 mg/kg/d for 2 days.

Bone Histomorphometry

Table 1 shows the results of histomorphometric parameters from pre-BP treatment transiliac bone samples of patients 3 (male) and 5 (female). Histological images are depicted for both patients and a control in **Figure 1a-1c.** The cortex was the most abnormal structural bone parameter in biopsy samples of Patients 3 and 5. Cortical width was 55 % of the mean for age in Patient 5. The cortices in Patient 3 appeared highly porous or trabecularized with no clear distinction between the cancellous and cortical compartment to the extent that cortical width was not measurable (**Figure 1a**). Trabecular number and cancellous bone volume was elevated only in patient 3, but average for age in patient 5. There was no hyperosteocytosis. Patient 5's trabecular compartment contained a few areas with woven bone nodules (**Figure 1d**) but the large majority of trabeculae consisted of lamellar bone.

Static parameters of bone formation showed that osteoblast surface/bone surface was 320 % and 170 % of the mean for age in patient 3 and 5, respectively. Osteoid thickness was above the reference range for age in Patient 5, but normal in patient 3. Dynamic parameters of bone formation showed inconsistent findings: patient 3's sample had a clearly elevated mineralization surface/bone surface and bone formation rate whilst these parameters were within the normal range in patient 5's sample. There was no mineralization defect in either of the patients.

Consistent in both samples was evidence for high bone resorption activity. Eroded surface was 183 % and 176 % of the mean for age in Patient 3 and 5, and the number of osteoclasts was 200 % and 175 %, respectively.

Patient 1's pre-treatment and patient 4's 20-months post-treatment bone biopsies were reported to show high bone resorption, but biopsies were not available for systematic histomorphometric analysis.

Bone mineralization density distribution (BMDD) (**Table 2, Figure 2**)

Quantitative Backscattered images from Patient 3 revealed highly trabecularized cortices **(Figure 2a)** which was not observed in Patient 5 **(Figure 2 b)**.

Trabecular Bone

Cancellous bone from patients 3 and 5 showed a slight tendency towards higher matrix mineralization as mirrored by the peak position (CaPeak) of the BMDD (**Figures 2c,d**). CaWidth was elevated, demonstrating greater heterogeneity in mineralization, with increased percentage of poorly mineralized bone (CaLow) in both patients, and increased percentage of highly mineralized bone (CaHigh) in Patient 5 (**Table 2**), compared to reference populations (26).

Cortical Bone

The CaPeak position of patient 3 was in the normal range, but slightly shifted towards lower bone matrix mineralization in patient 5, compared to controls **(Figures 2e,2f)**. CaWidth was again elevated, demonstrating greater heterogeneity in mineralisation, with increased percentage of highly mineralized bone (CaHigh) in both samples, and a greater percentage of poorly mineralized bone (CaLow) in patient 5, compared to reference population (26). (**Table2**).

Lumbar spine bone density before and during BP treatment

Age-, gender-, and size-adjusted lumbar spine bone density Z-scores (BMAD, HAZ) were below average before treatment in all patients, ranging from -0.5 to -3.4 (median–1.3). These Z-scores increased during BP treatment, with median ΔZ-score of +0.7 (0.1 to 1) after 1 year of treatment and a peak change of +1.5 (0.1 to 3.3) during treatment. However, after discontinuation of treatment HAZ dropped again from 0.3 to -2.5 in Patient 2, and from -0.7 to -1.1 in patient 3 (**Figure 3**). BP treatment was not restarted in patient 2 due to multiple dental procedures. Patient 4 had the greatest initial increase in rise in BMD, which was not sustained on oral alendronate. His BMD dropped after each BP treatment discontinuation but his clinical course was also complicated by progressive renal failure.

pQCT results before and during BP treatment

Table 3 demonstrates pQCT data at baseline (patients 1, 3 and 5), during zoledronate therapy (patients 1, 3) and following its discontinuation (patient 3). The common characteristic baseline feature of all three patients is the very low cortical density Z-score (-4.3, -4.9, -3.7, respectively), as well as low cortical thickness (-2.3, -1.1, -2.3, respectively). During zoledronate therapy, cortical density increased in both patients (patient 1: 984 mg/cm^3 to 1022 mg/cm^3, patient 3: 885 mg/cm^3 to 1029 mg/cm^3), although patient 1's value did not increase relative to reference data (Z-score pre-treatment: -4.3, after 4 years of treatment: -4.9). Patient 3's cortical density continued to improve even after the discontinuation of zoledronate (Z-score -2.5). Cortical thickness Z-score increased significantly with treatment in patients 1 and 3 and decreased again in patient 3 following treatment discontinuation. In contrast to the low cortical bone thickness and density at the proximal radius, trabecular and total bone density at the distal radius were relatively normal. Surprisingly, total and trabecular density Z-scores decreased during BP therapy in patient 1 but increased in patient 3, and dropped to very low levels after treatment discontinuation.

Fractures and progress of acroosteolysis

At start of BP therapy, patients 1, 3 and 5 had multiple vertebral fractures and patients 1 and 2 had long bone fractures (P1: tibia/fibula, P2: radius/ulna) whilst patient 4 had no fractures. During therapy, patient 4 developed vertebral and metatarsal fractures and patient 3 sustained a tibia fracture, while P1 and P2 sustained no new fractures. Patient 2 developed fractures of fingers and metatarsals after treatment cessation. Mild undertubulation of the metaphyses were observed in patient 2 during treatment, and as treatment did not appear to slow the progression of acroosteolysis, BP therapy was paused. The forth fingers were spared bilaterally. Since reaching skeletal maturity, acroosteolysis has remained stable (currently aged 21y). In contrast, patient 4 showed slower progression of acroosteolysis during BP treatment, compared to before treatment. No details are available on the progression of acroosteolysis in patients 1, 3 or 5.

Discussion

The results of this study indicate a unique bone tissue phenotype of patients with HJCYS, characterized by increased bone resorption, with or without increased trabecular bone formation, a greater than normal heterogeneity in mineralization, and immature, woven bone. Structurally, activating *NOTCH2* mutations appear to affect appendicular cortical bone more than trabecular bone. The markedly reduced cortical thickness and density and lumbar spine BMD increase substantially in response to BP therapy, indicating that affected individuals benefit from anti-resorptive therapy. This report also adds three novel *NOTCH2* mutations to the literature.

Limited bone histological analyses from affected adults have highlighted HJCYS as a form of high turnover osteoporosis, but the older literature is inconclusive (11-14,27). Increased bone resorption certainly was a hallmark finding in tissue samples of our patients. Elevated resorption markers were previously reported in HJCYS subjects (14). Bone formation appeared less affected than resorption in histomorphometric analysis. In fact, while patient 5 had normal static and dynamic parameters of bone formation, patient 3 had elevated amounts of trabecular bone with increased bone formation. Decreased trabecular bone volume was previously only described in very young HJCYS mouse mutants who show no defect in OB differentiation or their bone-forming capacity *in vitro* from age 3 months (10). Hence, the predominantly cortical rather than trabecular bone defect we observed may be a result of compartment-specific differential regulation by Notch signalling (10), with increased endocortical bone resorption leading to thinning and trabecularisation of the cortices. Alternatively, the normal or increased trabecular numbers could potentially be a biomechanical compensation for reduced cortical bone, or the result of variable expressivity of modifier genes.

Apart from excessive bone resorption, the other common feature was the more heterogeneous matrix mineralization, caused by variably increased proportions of poorly and/or highly mineralized bone in both cortical and trabecular bone. Despite normal or increased bone formation, matrix mineralization in cancellous bone was slightly right-shifted (towards higher mineral content of the bone matrix) rather than left-shifted, as one would expect with high bone turnover (25). Possibly, the increased

matrix mineralization heterogeneity might be due to the presence of densely mineralized woven bone within normal bone tissue (34,35). Indeed, patient 5 was found to have immature, woven bone, a finding previously described in a maxillary bone specimen from patient 2 when he was 14 years old (27). The presence of woven bone likely represents a typical feature of *NOTCH2*-mutated bone, since it is also present in *Notch2*-mutated mice and associated with increased proliferation of immature osteoblasts (36).

The most striking new finding on bone imaging was the uniformly low cortical thickness and density in all patients undergoing pQCT scanning (n=3), which is consistent with the trabecularization of the cortex seen on biopsy. Low cortical thickness and high cortical porosity are also features of the *Notch2*-mutated mouse (10). This finding fits the histologically evident excessive resorption rather than a formation defect, a hypothesis supported by observation of increasing cortical thickness during BP therapy in this study.

The increased osteoclast number and bone resorption in mice with activating *HJCYSNotch2* mutations is in accordance with our histomorphometric findings. However, Patient 3 had increased trabecular bone and trabecularization of the cortex as reported in the appendicular skeleton of mouse models with OB-specific Notch2 inactivation (37,38). This counterintuitive result gives rise to speculation of variable gene expressivity and post-receptor interactions in osteoblast and osteoclasts. In addition, age and gender may also play a role, as demonstrated in mouse models (37,39). Of note, Notch pathway activation in osteocytes leads to induction of Opg expression and Wnt/β-catenin signaling, with a consequent suppression of bone resorption in cancellous bone, and enhancement of bone formation in cortical bone (7).

The natural evolution of HJCYS leads to significant osteoporosis with vertebral compression fractures and continuous deterioration of acroosteolysis (11, 19, 40, 41). A previous report following 2 patients with HJCYS for 17 years without any treatment, showed a dramatic decrease in height and chronic back pain due to progression of vertebral fractures, alongside a decrease in BMD. The progression of

acroosteolysis continued during follow-up (11). The mechanism of disease for acroosteolysis in HJCYS is poorly understood. Samples containing acroosteolysis showed increased osteoclastic bone resorption and reduced bone formation (14) whilst others had high numbers of mast cells and neovascularisation with absent osteoclasts (12, 42). Acroosteolysis seemed to progress in patient 2 despite BP therapy and plateaued post puberty but showed slower progression in patient 4, reinforcing the suggestion of a disease mechanism other than osteoclastic bone resorption (21).

There are no controlled trials on the management of osteoporosis in HJCYS, apart from anecdotal cases treated with BPs, teriparatide or denosumab (15-20). Taking into consideration that elevated bone resorption is the main feature in the pathogenesis of osteoporosis in HJCYS, BPs are the logical therapeutic option in these patients, as they lead to osteoclast apoptosis (43). Accordingly, BPs have become the primary therapy for managing skeletal conditions characterized by increased osteoclast-mediated bone resorption. Here, we show the improvement in height-adjusted lumbar spine BMD z-scores and cortical thickness in treated patients. However, relatively fast reversibility of treatment benefit was observed soon after treatment discontinuation as demonstrated in patients 2 (by DXA), 3 (by DXA and pQCT) and 4 (by DXA and post-BP biopsy). This reversibility appears more pronounced compared to data from children with osteogenesis imperfecta (44). The BMD increase during BP treatment is in accordance with most cases of BP therapy in adults (16,17), apart from one case where glucocorticoids were co-administered (15). In children with HJCYS, there are only two case reports of intravenous BP therapy, which showed substantial improvement in lumbar spine BMD, a 9 % gain over 1 year in a 13-year old boy (21) and 67 % gain over 2 years in a 9-year old girl (20). Bone resorption markers also decrease during BP therapy (15,16). Overall, the results of this study and the existing literature support the use of intravenous BP therapy in patients with HJCYS. Given the association of HJCYS with renal disease (1) and the nephrotoxicity of zoledronate, renal function should be monitored during BP therapy. Anti-resorptive therapy with denosumab may also be beneficial (18).

While it is reasonable to assume that fracture risk decreases during BP therapy, such evidence will be difficult to collect in such an ultra-rare disease. Treatment guidelines on type and duration of anti-resorptive therapy will need to be established, including systematic observation of acroosteolysis, in a rare bone disease registry. HJCYS clearly is a multi-system disorder, demonstrating that *NOTCH2* activation affects development and function of several organs.

In conclusion, this study demonstrates increased bone resorption, increased heterogeneity of bone matrix mineralization, woven bone, and reduced cortical thickness as typical bone characteristics of HJCYS. These features are consistent with the effect of presumptive activating *NOTCH2* mutations on osteoclastogenesis and cortical bone described in mouse models. Here, we demonstrate that intravenous BP therapy increased size-corrected lumbar spine BMD and radial cortical thickness and density, which provides further evidence of beneficial treatment effects in children with HJCYS. Since treatment effects were not sustained after BP discontinuation, further studies are needed to inform guidance on treatment dose and duration. Whether acroosteolysis can be improved with BP therapy remains to be elucidated. From a clinical management perspective, the bone phenotype of our patients at baseline suggests, similar to other paediatric conditions with high bone resorption, that early diagnosis, including assessment for vertebral fractures, is essential so that therapy can be started earlier in life.

Acknowledgements

We thank Nicola Crabtree for assisting in interpretation of pQCT and DXA scans, and Daniela Gabriel, Petra Keplinger, Sonja Lueger and Phaedra Messmer for careful sample preparations and qBEI measurements at the bone laboratory of the Ludwig Boltzmann Institute of Osteology in Vienna. This study was supported [in part] by the Intramural Research Program of the NIH, NIDCR; AUVA (Research funds of the Austrian workers´ compensation board); WGKK (Vienna Regional Health Insurance Fund), and the Shriners of North America. MS was supported by Genome Canada, Genome Quebec and the Centre de Recherche du CHU Ste-Justine.

References

1. Canalis E, Zanotti S. Hajdu-Cheney syndrome, a disease associated with *NOTCH2* mutations. Curr Osteoporos Rep. 2016;14:126-131.
2. Hajdu N, Kauntze R. Cranio-skeletal dysplasia. Br J Radiol. 1948;21(241):42-8.
3. Cheney WD. Acro-osteolysis. Am J Roentgenol Radium Ther Nucl Med. 1965;94:595-607.
4. Isidor B, Lindenbaum P, Pichon O, Bezieau S, Dina C, Jacquemont S, Martin-Coignard D, Thauvin-Robinet C, Le Merrer M, Mandel JL, David A, Faivre L, Cormier-Daire V, Redon R, Le Caignec C. Truncating mutations in the last exon of NOTCH2 cause a rare skeletal disorder with osteoporosis. Nat Genet. 2011;43(4):306–8.
5. Simpson MA, Irving MD, Asilmaz E, Gray MJ, Dafou D, Elmslie FV, Mansour S, Holder SE, Brain CE, Burton BK, Kim KH, Pauli RM, Aftimos S, Stewart H, Kim CA, Holder-Espinasse M, Robertson SP, Drake WM, Trembath RC. Mutations in NOTCH2 cause Hajdu-Cheney syndrome, a disorder of severe and progressive bone loss. Nat Genet 2011;43(4):303–5.
6. Canalis E, Adams DJ, Boskey A, Parker K, Kranz L, Zanotti S. Notch Signaling in Osteocytes Differentially Regulates Cancellous and Cortical Bone Remodeling. J Biol Chem. 2013 Aug 30; 288(35): 25614–25625.
7. Majewski J, Schwartzentruber JA, Caqueret A, Patry L, Marcadier J, Fryns JP, Boycott KM, Ste-Marie LG, McKiernan FE, Marik I, Van Esch H; FORGE Canada Consortium, Michaud JL, Samuels ME. Mutations in NOTCH2 in families with Hajdu-Cheney syndrome. Hum Mutat. 2011;32(10):1114–7.
8. Regan J, Long F. Notch signalling and bone remodelling. Curr Osteoporos Rep. 2013;11(2):126-129.
9. Zanotti S, Canalis E. Notch and the Skeleton. Mol Cell Biol. 2010;30:886–896.
10. Canalis E, Schilling L, Yee SP, Lee SK, Zanotti S. Hajdu Cheney mouse mutants exhibit osteopenia, increased osteoclastogenesis and bone resorption. J Biol Chem. 2016;291(4):1538–51.

11. Leidig-Bruckner G, Pfeilschifter J, Penning N, Limberg B, Priemel M, Delling G, Ziegler R. Severe osteoporosis in familial Hajdu-Cheney syndrome: progression of acro-osteolysis and osteoporosis during long-term follow-up. J Bone Miner Res. 1999;14(12):2036-41.
12. Udell J, Schumacher HR, Kaplan F, Fallon MD. Idiopathic familial acroosteolysis: Histomorphometric study of bone and literature review of the Hajdu–Cheney syndrome. Arthritis Rheum 1986;29:1032–1038.
13. Brown DM, Bradford DS, Gorlin RJ, Desnick RJ, Langer LO, Jowsey J, Sauk JJ. The acroosteolysis syndrome: morphologic and biochemical studies. J Pediatr. 1976;88(4 Pt 1):573-580.
14. Nunziata V, di Giovanni G, Ballanti P, Bonucci E. High turnover osteoporosis in acro-osteolysis (Hajdu-Cheney syndrome). J Endocrinol Invest 1990;13: 251-255.
15. Hwang S, Shin DY, Moon SH, Lee EJ, Lim SK, Kim OH, Rhee Y. Effect of zoledronic acid on acro-osteolysis and osteoporosis in a patient with Hajdu-Cheney syndrome. Yonsei Med J. 2011;52(3):543-6.
16. Drake WM, Hiorns MP, Kendler DL. Hadju-Cheney syndrome: response to therapy with bisphosphonates in two patients. J Bone Miner Res. 2003;18(1):131-3.
17. McKiernan FE. Integrated anti-remodeling and anabolic therapy for the osteoporosis of Hajdu-Cheney syndrome: 2-year follow-up. Osteoporos Int. 2008;19(3):379-80.
18. Adami G, Rossini M, Gatti D, Orsolini G, Idolazzi L, Viapiana O, Scarpa A, Canalis E. Hajdu Cheney Syndrome; report of a novel NOTCH2 mutation and treatment with denosumab. Bone. 2016;92:150-156.
19. Deprouw C, Feydy A, Giraudet Le Quintrec JS, Ruiz B, Kahan A, Allanore Y. A very rare cause of acro-osteolysis: Hajdu-Cheney syndrome. Joint Bone Spine. 2015;82(6):455-9.
20. Galli-Tsinopoulou A, Kyrgios I, Giza S, Giannopoulou EZ, Maggana I, Laliotis N. Two-year cyclic infusion of pamidronate improves bone mass density and eliminates risk of fractures in a girl with osteoporosis due to Hajdu-Cheney syndrome. Minerva Endocrinol. 2012;37(3):283-9.
21. Lifchus-Ascher RJ, Tucci JR. Hajdu-Cheney syndrome in a 19-year-old man. Endocr Pract. 2006;12(6):690-4.

22. Glorieux FH, Travers R, Taylor A, Bowen JR, Rauch F, Norman M, Parfitt AM. Normative data for iliac bone histomorphometry in growing children. Bone 2000; 26:103–109.
23. Rauch F, Travers R, Glorieux FH. Intracortical remodeling during human bone development – a histomorphometric study. Bone 2007; 40:274–280.
24. Roschger P, Fratzl P, Eschberger J, Klaushofer K. Validation of quantitative backscattered electron imaging for the measurement of mineral density distribution in human bone biopsies. Bone 1998;23(4):319-26.
25. Roschger P, Paschalis EP, Fratzl P, Klaushofer K. Bone mineralization density distribution in health and disease. Bone 2008;42(3):456-66.
26. Fratzl-Zelman N, Roschger P, Misof BM, Pfeffer S, Glorieux FH, Klaushofer K, Rauch F. Normative data on mineralization density distribution in iliac bone biopsies of children, adolescents and young adults. Bone 2009;44:1043-1048.
27. Zhao W, Petit E, Gafni RI, Collins MT, Robey PG, Seton M, Miller KK, Mannstadt M. Mutations in NOTCH2 in patients with Hajdu-Cheney syndrome. Osteoporos Int. 2013;24(8):2275-81.
28. Carter DR, Bouxsein ML, Marcus R. New approaches for interpreting projected bone densitometry data. J Bone Miner Res 1992;7(2):137-45.
29. Zemel BS, Leonard MB, Kelly A, Lappe JM, Gilsanz V, Oberfield S, Mahboubi S, Shepherd JA, Hangartner TN, Frederick MM, Winer KK, Kalkwarf HJ. Height adjustment in assessing dual energy x-ray absorptiometry measurements of bone mass and density in children. J Clin Endocrinol Metab 2010;95(3):1265-73.
30. Rauch F, Schönau E. Peripheral quantitative computed tomography of the distal radius in young subjects - new reference data and interpretation of results. J Musculoskelet Neuronal Interact 2005;5(2):119-26.
31. Schoenau E, Neu CM, Rauch F, Manz F. Gender-specific pubertal changes in volumetric cortical bone mineral density at the proximal radius. Bone 2002;31:110–3.

32. Rauch F, Schoenau E. Peripheral quantitative computed tomography of the proximal radius in young subjects--new reference data and interpretation of results. J Musculoskelet Neuronal Interact 2008;8(3):217-26.
33. Brennan A.M, Pauli R.M. Hajdu-Cheney Syndrome: Evolution of phenotype and clinical problems. Am J Med Gen 2001;100:292-310.
34. Manjubala I, Liu Y, Epari DR, Roschger P, Schell H, Fratzl P, Duda GN. Spatial and temporal variations of mechanical properties and mineral content of the external callus during bone healing. Bone 2009;45(2):185-92.
35. Wagermaier W, Klaushofer K, Fratzl P. Fragility of bone material controlled by internal interfaces. Calcif Tissue Int 2015;97:201-212.
36. Engin F, Yao Z, Yang T, Zhou G, Bertin T, Jiang MM, Chen Y, Wang L, Zheng H, Sutton RE, Boyce BF, Lee B. Dimorphic effects of Notch signaling in bone homeostasis. Nat Med. 2008; 14:299–305.
37. Yorgan T, Vollersen N, Riedel C, Jeschke A, Peters S, Busse B, Amling M, Schinke T. Osteoblast-specific Notch2 inactivation causes increased trabecular bone mass at specific sites of the appendicular skeleton. Bone 2016;87:136-46.
38. Hilton MJ, Tu X, Wu X, Bai S, Zhao H, Kobayashi T, Kronenberg HM, Teitelbaum SL, Ross FP, Kopan R, Long F. Notch signaling maintains bone marrow mesenchymal progenitors by suppressing osteoblast differentiation. Nat Med 2008;14(3):306-14.
39. Canalis E, Schilling L, Zanotti S. Effects of Sex and Notch Signaling on the Osteocyte Cell Pool. J Cell Physiol 2017;232(2):363-370.
40. Stathopoulos IP, Trovas G, Lampropoulou-Adamidou K, Koromila T, Kollia P, Papaioannou NA, Lyritis G. Severe osteoporosis and mutation in NOTCH2 gene in a woman with Hajdu-Cheney syndrome. Bone. 2013;52(1):366-71.
41. Narumi Y, Min BJ, Shimizu K, Kazukawa I, Sameshima K, Nakamura K, Kosho T, Rhee Y, Chung YS, Kim OH, Fukushima Y, Park WY, Nishimura G. Clinical Consequences in Truncating Mutations in Exon 34 of NOTCH2: Report of Six Patients With Hajdu–Cheney

Syndrome and a Patient With Serpentine Fibula Polycystic Kidney Syndrome. Am J Med Genet Part A 2013;161A:518–526.

42. Elias AN, Pinals RS, Anderson HC, Gould LV, Streeten DH. Hereditary osteodysplasia with acro-osteolysis (the Hajdu-Cheney syndrome). Am J Med 1978;65:627-636.

43. Drake MT, Clarke BL, Khosla S. Bisphosphonates: mechanism of action and role in clinical practice. Mayo Clin Proc 2008;83(9):1032-45.

44. Rauch F, Munns C, Land C, Glorieux, FH. Pamidronate in Children and Adolescents with Osteogenesis Imperfecta: Effect of Treatment Discontinuation. J Clin Endocrinol Metab 2006;91(4):1268-1274.

Figure Legends:

Figure 1. Histological images (Goldner Trichome staining) from transiliac bone biopsies naïve to bisphosphonate therapy. a) Patient 3 (male, 15y): note increased trabecular density compared to control and trabecularization of the cortex (arrow); b) Patient 5 (female, 10y): note the relatively thin cortex and normal trabecular bone, c) Healthy control sample (female, 9.4y); d.) Patient 5: note the presence of woven bone (arrow) which is atypical in this location.

Figure 2. Quantitative backscattered images depicting cortical dimensions and trabecular network (a,b), and BMDD histograms of cancellous (c,d) and cortical bone (e,f) from transiliac biopsy samples of patient 3 (left panels) and 5 (right panels). BMDD results of cancellous and cortical bone are compared to reference BMDD from healthy children (gray band) (26). The corresponding parameters are given in Table 2.

Figure 3. Age-, gender- and size-adjusted lumbar spine BMD Z-scores in response to bisphosphonate therapy in Patients 1-4. BMAD Z-scores are used for patients measured on Lunar scanners and HAZ for patients on Hologic scanners. Arrows pointing downwards indicate treatment discontinuation, arrows pointing upwards treatment restart. For details on dose and choice of bisphosphonate therapy please refer to text.

Table Legend:

Table 2: CaMean, the weighted mean calcium concentration of the bone area; CaPeak, the peak position of the histogram that indicates the most frequently occurring calcium concentration of the bone area; CaWidth, the full width at half maximum of the distribution, describing the variation in mineralization density; CaLow, fraction of poorly mineralized bone area defined as the percentage of the area below 17.68 wt% Ca, corresponding to the 5th percentile of adult reference BMDD; CaHigh, fraction of highly mineralized bone defined as the percentage of bone area that is

mineralized above 25.30 wt% Ca, corresponding to the 95th percentile of the adult reference range) (25). Reference data are mean (±1SD) or median with interquartile range [25%; 75%].

Figure 1

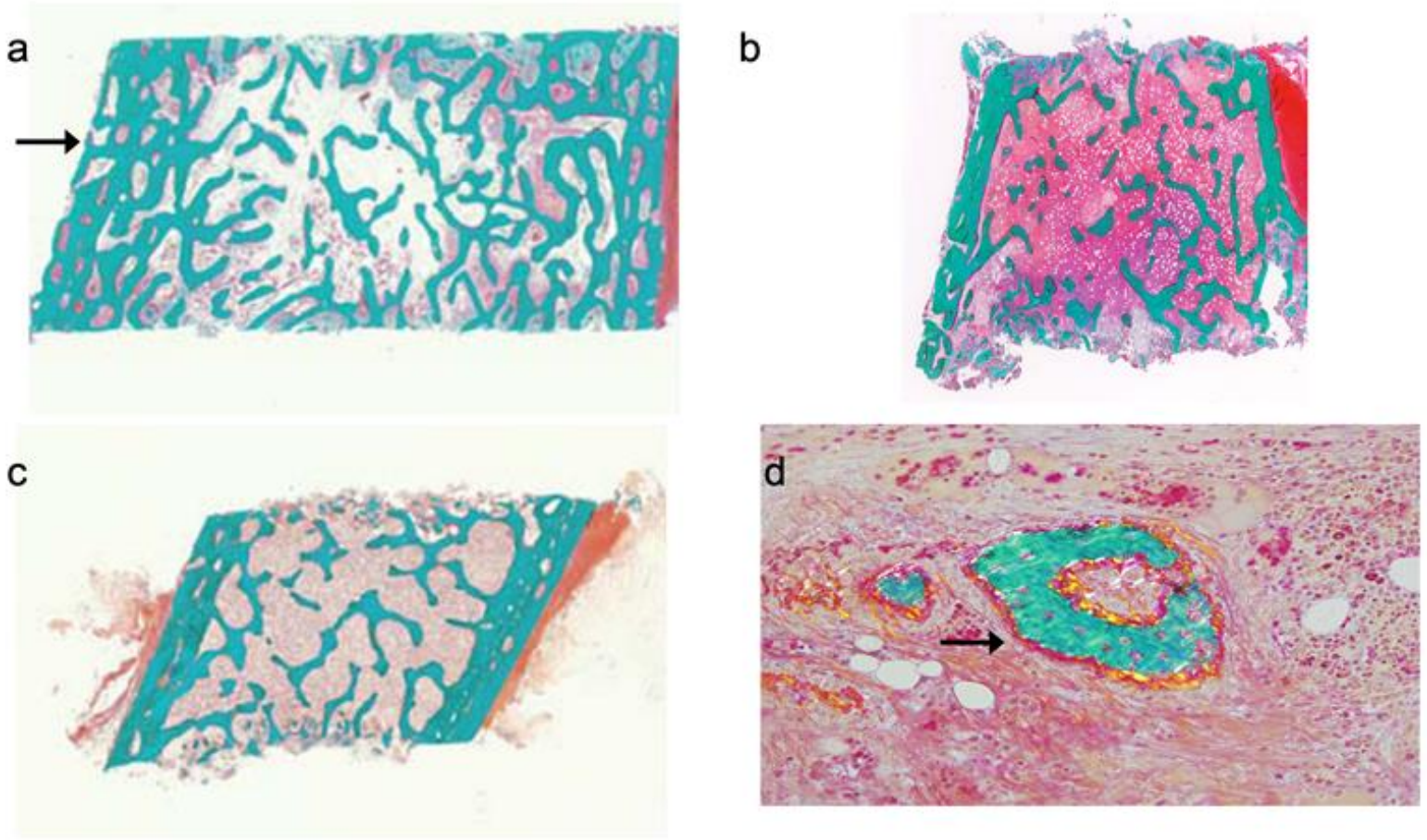

Figure 2

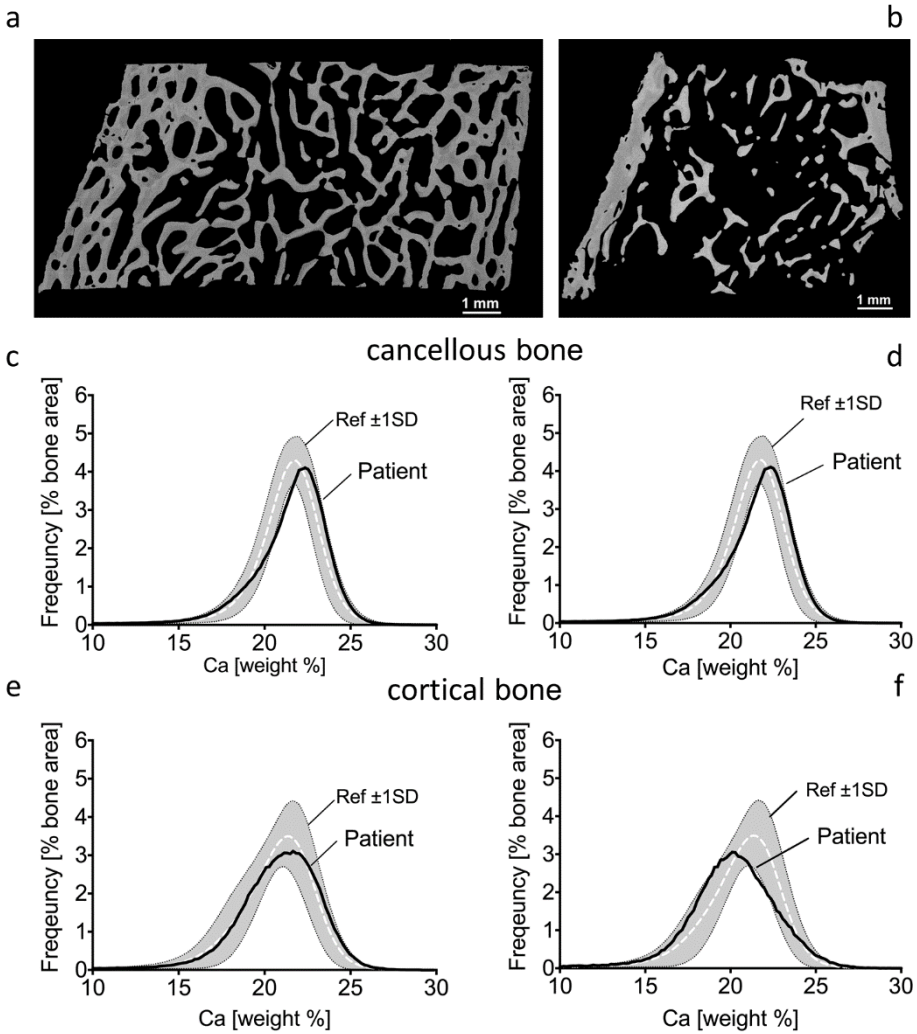
a
b
1 mm
1 mm
cancellous bone
c
d
Freqeuncy [% bone area]
Ref ±1SD
Patient
Ca [weight %]
cortical bone
e
f

Figure 3

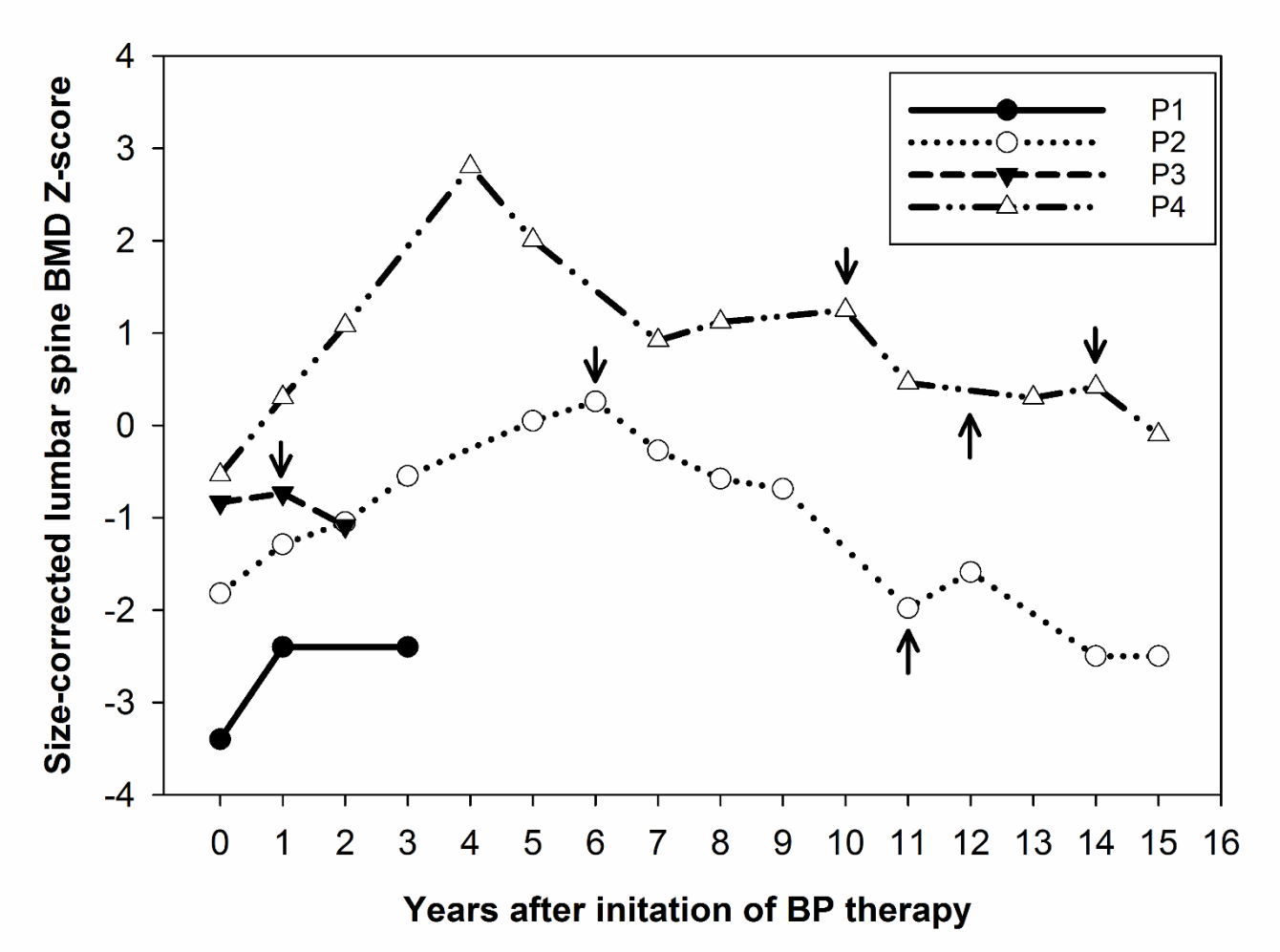
Size-corrected lumbar spine BMD Z-score
4
3
2
1
0
-1
-2
-3
-4
0 1 2 3 4 5 6 7 8 9 10 11 12 13 14 15 16
Years after initation of BP therapy
P1
P2
P3
P4